INFN Istituto Nazionale di Fisica Nucleare
LABORATORI NAZIONALI DI FRASCATI
SIS-Pubblicazioni

LNF–07/11(P)
April 16, 2007

X-BAND RF STRUCTURE THERMAL ANALYSIS AND TESTS

S. Bini[1], V. Chimenti[1], L. Palumbo[2], B. Spataro[1], L.Quintieri[1], F. Tazzioli[1] *
[1)] *INFN-Laboratori Nazionali di Frascati, 00044 Frascati (RM), Italy*
[2)] *Dipartimento di Energetica- Facoltà di Ingegneria, Università La Sapienza, 00161 Roma Italy*

Abstract

The design of X-band multi-cell RF structures for particle accelerators requires an accurate estimation of the sensitivity to the mechanical deformations induced by the surface power loss on the metallic walls. The prediction of these effects is important for conceiving a tuning strategy that assures the correct structure operation when integrated into the accelerator complex. An experimental technique is proposed for preliminary testing of the mechanical deformations caused by a thermal load that can generate in the RF cavity a temperature gradient profile as close as possible to the real one induced by the electromagnetic power loss. Because we want to find a method that can be easily and cheaply implemented in the laboratory, a thermal radiator with uniform heating power density, placed on the axis of the RF cavity, has been chosen as heating source. A multi-physics finite-element code (ANSYS) has allowed comparing the measured temperature gradients with the computed ones. The good agreement validates the application of the code, which has been extended to the joint solution of the electromagnetic and thermal problem. Thus the sensitivity to deformations can be directly evaluated.

Keyword: x-band, RF structure, thermal computing
PACS: 29.17, +w, 07.05.T_p

Submitted to Nucl. Instr. and Meth. In Phys. Res. A

* Corresponding author: e-mail address: Franco.Tazzioli@lnf.infn.it

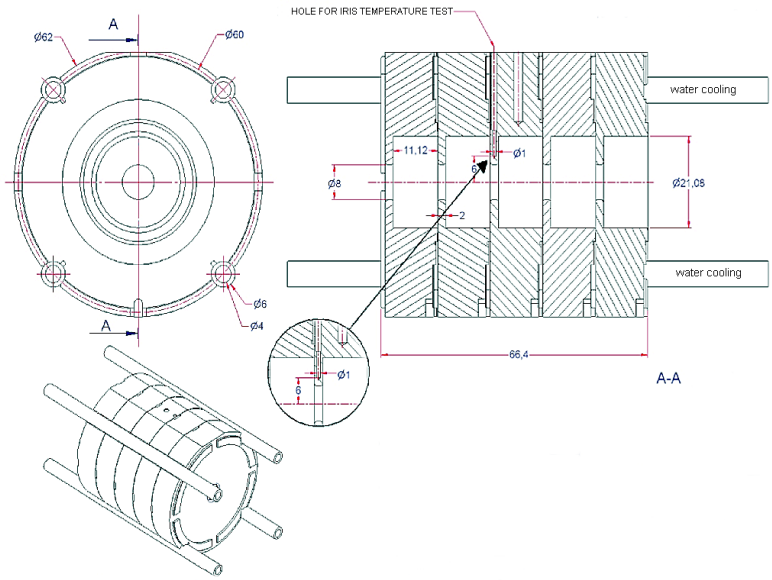

Figure 1: Eperimental set-up

1 Introduction

This paper presents the thermal power tests and the relative computations on a partial model of an 11.4 GHz compact standing wave π-mode structure required to improve the beam brightness in the SPARC advanced photo-injector [1]. The average power dissipation in the full 9 cells structure will be 300 W, that is 33 W per cell. Considering the compactness of the structure, this is a remarkable power level. Therefore detailed thermal information on the behavior of the accelerating section is necessary. The knowledge of the equilibrium average temperature as well as its distribution is important since they influence the cell dimensions and therefore the resonant frequencies of the electromagnetic modes. RF power tests on a prototype model would imply the full implementation of the RF coupler and the availability of a high average power X-band RF source. We have devised a test set up that circumvents this difficulty and gives an approximate evaluation of the thermal behavior of the structure. A brazed Copper five cells prototype has been built and thermal experiments have been performed. A thermal radiator with uniform heating power density, placed on the axis of the RF cavity, has been chosen as heating source. The structure is shown in Figure 1. By means of a water-cooling system made with four copper tubes, parallel to the axis, in contact with the outer surface, connected in serial mode, the external temperature can be controlled. The maximum inner temperature is expected to be on the irises. This paper presents results related to experimental measure-

ments of temperature gradients. These results are then compared with those coming from numerical computation.

In the computational section this paper reports:

- The comparison between measurements of the temperature profile in a RF cavity heated by a thermal radiator, documented in [2] and numerical simulations of the experimental cases (using ANSYS finite element code), for several input powers.

- The comparison between the estimated temperature distribution and mechanical strain and stress field, inside the cavity, in the case of radiation heating and in the case of induced electromagnetic power loss, for the same input power. This is done because we want to check that the experimental data from this kind of measurements can be effectively used to foresee the actual thermal profile due to electromagnetic power loss.

Finite element analysis has been carried out using the *ANSYS* software[3]. *ANSYS* is a multi-physics environment that includes a High Frequency solver module and we use it to perform coupled analysis: RF-Thermal-Mechanical. The High Frequency module has for the moment the limitation that only 3D elements can be used, so 3D simulations have to be performed also for virtually 2D problems (e.g., axis-symmetric structures where the modes of interest are also symmetric around geometric axis).

The finite element analysis has been carried out in two steps:

- A 2D model has been used for evaluating the radiation heat exchange between the thermal radiator and the cavity. In addition the thermal strain field induced by the temperature profile in the structure, for steady-state condition, has been estimated. The results obtained from these calculations have been compared with the experimental values, giving a satisfactory agreement (accordance within 17% in the worst case), taking also into account the uncertainty on some material properties especially about the surface emissivity.

- A 3D model has been created for developing a coupled high-frequency electromagnetic and thermal analysis. The temperature profile has been calculated, supposing the cavity to be operating in continuous regime at the designed π-mode frequency (11.4 GHz).The magnetic field intensity has been chosen in order to perform a coherent comparison with the power heating used in the laboratory tests.

The main objective of this work is to demonstrate that it is possible to use a thermal radiator for testing the temperature distribution and the consequent stress and strain field inside the cavity to estimate how much the induced mechanical deformation can affect the

frequency of the cavity. The preliminary comparison shows that such alternative system could be effectively used and with some improvements could fully reproduce the real case.

2 Experimental setup and results

The heater has the same effective length as the copper structure (about 66 mm) and a diameter of 6 mm (the diameter of the irises is 8mm). It is held in place by steel end caps on both ends. A shield reduces the heat losses between the inside of the structure and the air. For the same reason an external shield is mounted on the outside of the structure in order to reduce heat losses by convection.

In order to measure as closely as possible the temperature of the central iris tip, a 1 mm diameter hole was drilled as shown in Figure 1, extending from the outside surface to 1 mm before the inner surface of the iris. The temperatures are measured by K-thermocouples (Chromel-Alumel). A very thin thermocouple was introduced down to the end of the hole to contact the metal close to the iris tip. The mantle temperature is obtained by fixing another thermocouple on the external surface of the structure, near the hole. Thus the transversal temperature gradient ΔT between the central iris tip and the external surface of the copper mantle can be measured. Two K-thermocouples are applied on the water inlet-outlet, in order to measure the heat power flux.

By introducing a thermal shield, in order to minimize the power dissipated in air by convection, at equilibrium the electrical power supplied by the heater should be entirely dissipated by the water flow. We have performed several measurements at different power levels and by varying the inlet temperature of the water at constant flow rate. The equilibrium copper temperature is recorded in order to measure ΔT between iris and external surface of the structure. The temperatures have been acquired by means of a system controlled by LABVIEW software.

A typical plot of measured temperature values versus time is shown in Figure 2. The time to obtain steady state is about 400 sec. With these experiments we have verified that, by increasing the heating power, while maintaining constant the water flow rate (about 14 g/s), the equilibrium temperature variations on the external mantle surface are less than 2 degrees, in accordance with computations. The equilibrium temperature difference between iris tip and mantle increases by about 2 degrees per 100 W. This temperature difference is practically independent of the inlet water temperature.

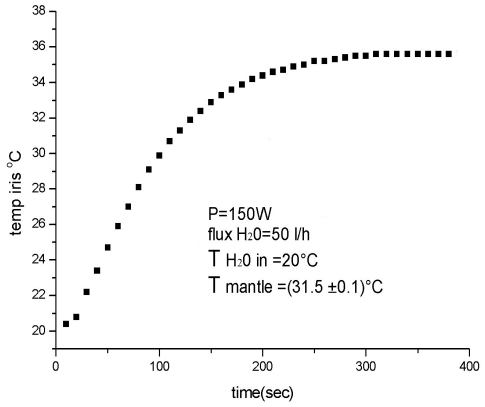

Figure 2: The iris temperature as a function of the time, data taken every 10 seconds. $T_{water} = 20^oC$

3 Thermal radiation calculation

The two-dimensional (2-D) finite element model used for the numerical simulation of the radiation heating is reported in Figure 3. The 2-D model has been built, taking advantage of the symmetry of geometry, loads and boundary condition. A plane axisymmetric element (plane 55), with a 2-D thermal conduction capability, has been used for meshing the geometric domain, with uniform mesh size, small enough to accurately reproduce high localized thermal and strain gradients (0.5 mm is the maximum element size for a total of 6877 elements).

The Physic Domain: The internal surface of these elements delimits the physic domain (that is the enclosure) for the radiation heat exchange. The enclosure in a radiation problem is a set of surfaces radiating to each other. ANSYS uses the definition of an enclosure to calculate view factors (the fraction of the radiation leaving surface *i* which is intercepted by surface *j*), amongst surfaces belonging to an enclosure. Each radiating surface has an emissivity and a direction of radiation assigned to it. The emissivity is a surface radiative property defined as the ratio of the radiation emitted by the surface to the radiation emitted by a black body at the same temperature. ANSYS restricts radiation exchange between surfaces to gray-diffuse surfaces, that signifies that emissivity and absorptivity of the surface do not depend on wavelength (either can depend on temperature) neither on direction. The emissivity for a surface can be a function of temperature and depends on the manufactured and oxidation state of the surface. In Table 1 the value of

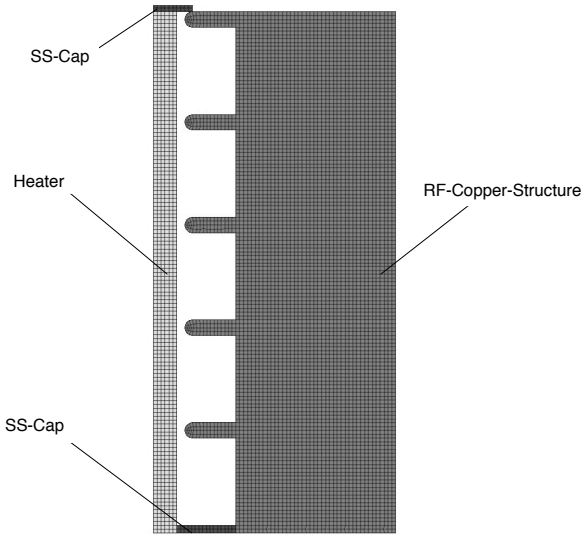

Figure 3: 2D Finite Element Model: the RF copper cavity, the ss caps and the heater

Table 1: Copper Emissivity

Surface State	Emissivity
commercial burnished	0.07
electrolytic polished	0.02
polished	0.031
polished annealed	0.008
oxidized	0.65
heavly oxidized	0.78
oxidized to black	0.88

copper emissivity for several surface status are reported. For the radiator an emissivity equal to 0.9 has been assumed, instead an inner surface emissivity of 0.11 has been considered for the stainless steel (polished-machine rolled ss). In our experiment the heating has been realized in air, so that the internal surface of the copper resulted oxidized and consequently, in order to reproduce thermal boundary conditions as much close as possible to the reality, a value of 0.7 (see Table 1) for the copper emissivity has been assumed for our calculations.

The Materials: The internal heater is a cylindrical bar of 6 mm diameter, made of a nichel-chrome alloy, whose thermal properties used in the calculation are reported in Table 2, together with the properties of oxygen-free copper of which the cavity is made. This heater is able to generate a power up to 400 W and is mounted on the axis of the

Table 2: Material Properties (in the temperature range 293-320 K)

Thermal properties	Ni-Cr-alloy	OF Copper
Density [kg/m^3]	8470.0	8960.0
Thermal Conductivity [W/mK]	11.4	388
Heat Capacity [J/kgK]	435.	383.
Thermal linear expansion	13.0E-6	16.4E-6

structure.

The Thermal Load: The aim of the calculation is to determine the temperature profile inside the cavity, due to the radiation heat exchange with the thermal heater. Consequently the induced mechanical deformations can be estimated, by means of a *sequentially coupled physics* approach. The thermal load has been applied in the elements of the radiator as an internal heat power generation. An initial uniform temperature has been specied to be about 293 K for the cavity and the radiator. For the calculation, conduction through the air inside the cavity has been also taken into account[1].

The Boundary Conditions: The boundary condition has been imposed by fixing the temperature on the external cavity surface, according to the measured steady-state values, for each input power applied. Anyway, in order to predict the maximum achievable ΔT in the cavity also in case of heat flow rates different from that experimentally used (i.e, heating power greater than 200 W), a convection heat exchange boundary condition has been introduced on the external nodes of the cavity, in such a way as to balance exactly the input power. In fact, because we want to estimate the stationary distribution of temperature, the net heat flow rate into the cavity has to be zero, otherwise the temperature profile would change with time.

The Numeric Solver: Because the radiation heat flow varies with the fourth power of the body's absolute temperature, radiation analyses are highly nonlinear. The numerical method used to simulate the radiation heat exchange is the *Radiosity* one that accounts for the heat exchange between radiating bodies by solving for the outgoing radiative flux for each surface, when the temperatures for all surfaces are known. The surface fluxes provide boundary conditions to the finite element model for the conduction process analysis.

The Results: The maximum radial temperature gradient in the cavity has been determined versus the input power in the radiator: the calculated values are compared with the measured ones in Table 3. As a result of this analysis we can conclude that the calculated values reproduce the experimental results within a 20% of average accuracy.

This level of precision can be considered satisfactory if we take into account the

[1]The air has been considered completely transparent respect to the radiation.

Table 3: Comparison between results from ANSYS simulation and measured values

Input Heat Rate [W]	Measured ΔT ± 0.2 [K]	Calculated ΔT [K]
60	1.	1.3
100	2.	2.15
150	4.	3.32

simplifying initial assumptions for the calculation. In fact, it is important to underline that in the 2D calculations the actual not uniform heat exchange by convection, on the external boundary surface, has been replaced or by a uniform fixed temperature condition or by a uniform convective heat exchange on the external surface[2], that surely contributes to have a flatter temperature profile. Furthermore, the temperature dependence of the thermal parameters in the material has been replaced by homogenous conditions by averaging the values over the temperature range.

On this basis, the comparison between the measured and the calculated values of temperature make us confident in having a validated 2D model for the radiation heat-exchange calculation, so that we can use it to do previsions.

In Figure 4 we report the estimated temperature field inside a completely symmetric cavity (with 6 irises, without end caps and with vacuum inside), when a 150 W radiating power is used to heat. The external boundary has been supposed to be cooled by a uniform convection as perviously described, supposing to have a water flow rate of 14 g/s with inlet temperature equal to 20^oC (according the experimental values). The corresponding estimation of the radial temperature profile at the position of the central iris (from the tip of the iris to the external cavity surface) is reported in in Figure 5.

The estimated axial temperature profile along the inner profile of the cylinder is shown in Figure 6: the temperature reaches a maximum on the the tip of each iris, as expected.

The axial temperature profile along the inner diameter of the cylinder (at the iris base) is shown in Figure 7: the temperature is symmetric around the middle of the cavity and the inner irises are hotter than the external ones. The not uniform longitudinal temperature profile can be explained by the fact that the six irises are not actually subjected to the same thermal loads: the inner ones are in fact warming little more than the two external ones. This is essentially due to the different view factors among the single cells composing the cavity in such a way that the external irises receive heating only from the

[2]The real convective-heat exchange inside the water tube surrounding the cavity is going to be accomplished and included as next step in the 3D complete model.

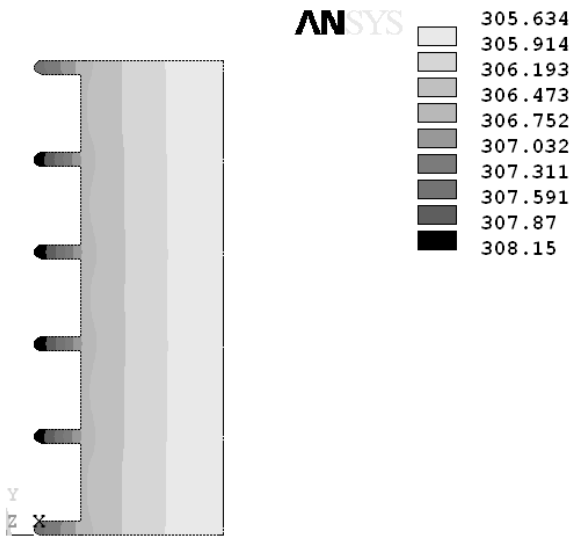

Figure 4: Temperature Field in the symmetric cavity for 150 W radiation heating

internal side. The maximum temperature on the two external irises is about 0.65 K lower with respect to the inner ones (40% of ΔT_{max}), where the maximum value of about 308 K is reached. This difference of temperature is reduced at about 1 tenth of degree (0.14 K) on the bulk material (see Figure 7).

4 Coupled thermo-structural and strain deformation calculation

In order to evaluate the strain induced by the temperature gradient we refer to a model of the cavity without end caps and having the mechanical constraints that the cavity should have when put in operation on the beam transfer line.The heating power (150W) has been supposed to be generated by means of an internal heater with uniform power density and, as it will be show later in this paper, the generated axial temperature profile (Figure 6 and 7) is similar to that calculated for the electromagnetic power loss. ANSYS allows the thermal elements to be converted directly to structural elements in order to obtain the stress and displacement solution. The thermal distortion of the cavity is evaluated on the basis of the thermal expansion coefficient of the material (see Table 2) and the nodal temperature data obtained from the thermal solution, that are applied as load on the structural model (according the sequential scheme for coupled calculations). Furthermore the symmetry boundary condition and the support constraints are included in the model. One end only is blocked: the cavity is free to expand. The initial temperature with respect

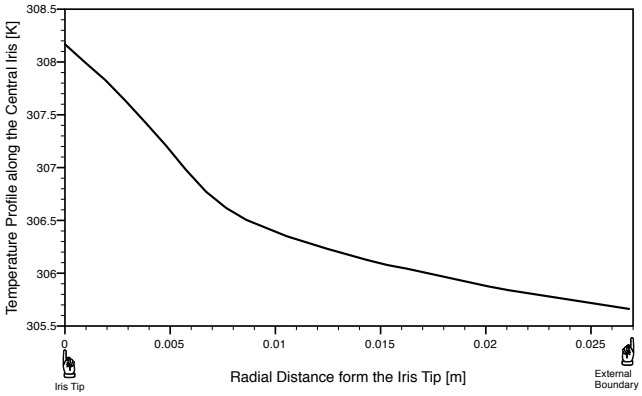

Figure 5: Radial Temperature Profile for 150 W radiation heating (from the tip of the central iris to the external cavity surface)

to which we estimate the thermal stress is the room temperature (i.e, T=293 K is the reference temperature at which the structure is supposed to be free of stress). In Figure 4 the total displacement is shown over the undeformed initial edges. Each cell of the cavity expands by a longitudinal total displacement of about 3.4 μm between two consecutive irises. The radial displacement is also quite uniform on all the cells and is about 2.5 μm.

The Von-Mises equivalent total strain and stress are shown in Figure 9: the maximum strain is located on the tips of the irises (0.61E-4) being the warmest regions in the cavity. The highest stresses in the cavity are caused by local thermal gradients between the hottest inner surface and the external cooled boundary and by the differential expansion of the warm regions with respect to the rest of the cavity. The maximum stress, on the tips of the irises, is equal to about 6.7 MPa (the yield stress in oxygen free copper is about 200 MPa).

5 The 3-dimensional Coupled Analysis: Electromagnetic-Thermal

The commercial finite-element code ANSYS provides the ability to link electromagnetic to thermal and structural analyses. For version after 5.4, Ansys provides the high-frequency (HF) analysis module and associate elements. This module has been applied in order to evaluate the RF loss and the consequent temperature distribution in our cavity. A coupled-field analysis by a unique code is more efficient respect to using different specialized software. In fact the exchange of information between electromagnetic field simulators and structural/thermal simulators can be difficult and can lead to errors. In case of multi-physics code like ANSYS this exchange of information between different

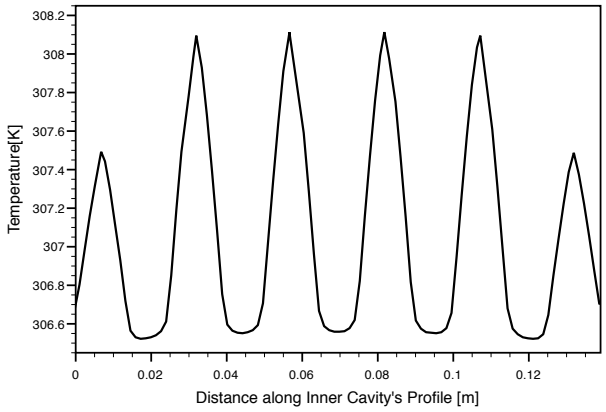

Figure 6: Axial Temperature Profile in the Cavity (along the inner profile of the cavity) in case of uniform radiation heating power density

modules is a built-in feature of the software, so that the model can be established by one single software and related data can be transferred more efficiently and easily between elements due to same mesh employed.

5.1 The 3D model

The initial phase of the analysis consists of a high frequency electromagnetic calculation on the inner vacuum volume. The model is composed of a solid 3-dimensional volume representing the inner vacuum of the cavity plus two short cylindrical volumes on the extremities (representing the vacuum volume of the beam-line). In order to reduce the CPU time for calculation, the model has been constructed taking advantage of symmetry conditions. Only 45 degrees of the whole structure has been meshed, using tetrahedral RF elements (HF119) with uniform fine mesh (for a total of 24575 elements only for the vacuum). HF119 is a high-frequency tetrahedral element which models 3-D electromagnetic fields and waves governed by the full set of Maxwell's equation in linear media. HF119 applies to the full-harmonic and modal analysis but not to the transient analysis. Even if the electromagnetic results are fairly insensitive to mesh density, however the surface heat flux is highly dependent on the mesh size at the cavity wall-to-vacuum boundary. A satisfactory mesh has been generated by an iterative process with the goal to have a heat flux on external boundary not depending on the mesh size (the magnetic fields at the surface and thus the surface heat fluxes are accurately depicted while minimizing CPU time and memory usage). Figure 5 shows the meshed vacuum volume used to obtain the electromagnetic solution. Electric wall conditions (electric field normal to the wall-to-

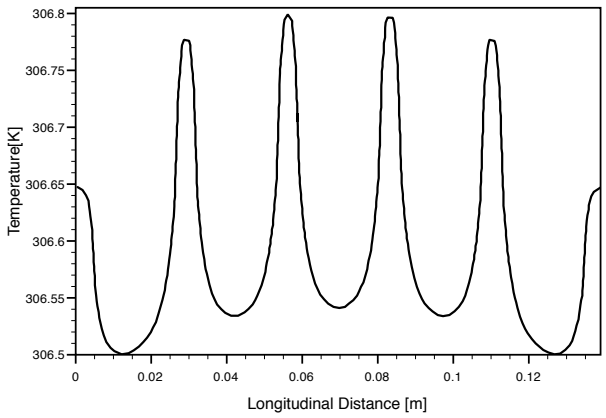

Figure 7: Axial Temperature Profile in the Cavity (along the inner diameter at the iris bases) in case of uniform radiation heating power density

vacuum surface) are applied to the exterior surface of the whole vacuum volume, whereas the impedance boundary conditions (surface resistivity) are applied only on the cavity interior surface like surface load (sf command with keyword '*shld*'). No boundary conditions have to be applied to the model's symmetry planes since in ANSYS unconstrained surfaces are set by default to magnetic walls.

5.2 High-Frequency Electromagnetic Calculation

The modal analysis allows to individuate the working frequency of the π-mode, for which we intend to develop the harmonic analysis. The natural modes of the cavity have been extracted between 10.5e+9 and 15.e+9 Hz using the Block Lanczos numerical solver[3]. We find in this frequency range 5 resonances. The electric field of the π-mode[4] (11.4 GHz) (in which we are interested) is reported in Figure 5.2. In order to evaluate the power loss induced in the skin depth of the copper surface, an harmonic excitation at 11.4 GHz working frequency has been applied to the cavity. This means that the cavity, in our calculations, is supposed to work in continuous regime at the π-mode. The excitation has been applied by using a suitable *modal* port, this being a new feature available on the last version of ANSYS (10.0).We applied the modal port load on the nodes of a plane surface in the center of one external cell of the cavity. The excitation of the resonance

[3]ANSYS calculates the element results in the form of normalized electric and magnetic field vectors and flux density vectors

[4]In order to compensate the amplitude of the electric field in all the cells of the resonant cavity, the inner radius of the outer ones has been reduced of about 60μm

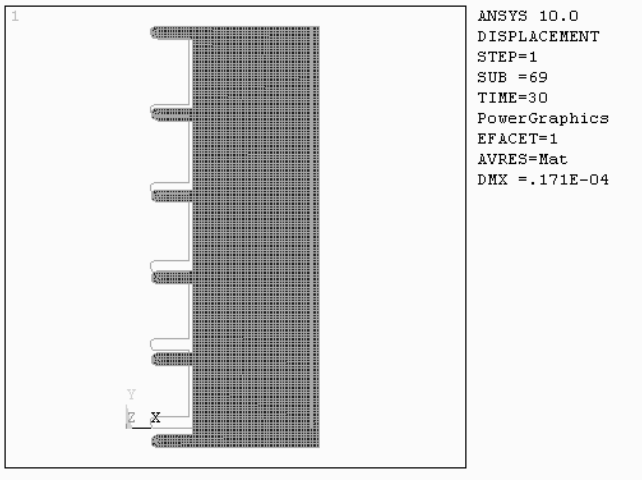

Figure 8: Total Displacement [m]

can be obtained for different values of the peak electric field, or in equivalent way, for different values of electromagnetic power stored per cycle in the cavity. We have chosen the first option and by means of interactive calculations we found the electromagnetic field corresponding to 37.5 W of power loss (a quarter of the whole structure only has been modeled), in order to compare these results with the case of 150 W supplied by radiation heating.

Among the output data obtainable from the electromagnetic solution output associated with the HF119 element, the following item is essentially used to derive the thermal load to be applied on the the vacuum-cavity interface nodes: *hflxavg*, that is the heat flow rate across the contact faces of the selected elements, caused by the surface losses in the copper skin.

We have written a macro that for each element that has, at least, a face in contact with the vacuum-cavity interface wall, extracts the heat flux value (the *hflxavg* output parameter). Finally the macro records these values in a table. With another macro we transfer the heat flow rate of each element as surface load on the nodes belonging to the inner wall of the cavity. Before launching the calculation we checked that the total sum on the inner surface of the *hflxavg* values in the table coincides exactly with the surface loss value, estimated by the macro *powerh*. This is a built-in macro that calculates the time-averaged (rms) power loss in a conductor or lossy dielectric material from a harmonic analysis. We can see the distribution of the calculated thermal heat flux in Figure 12.

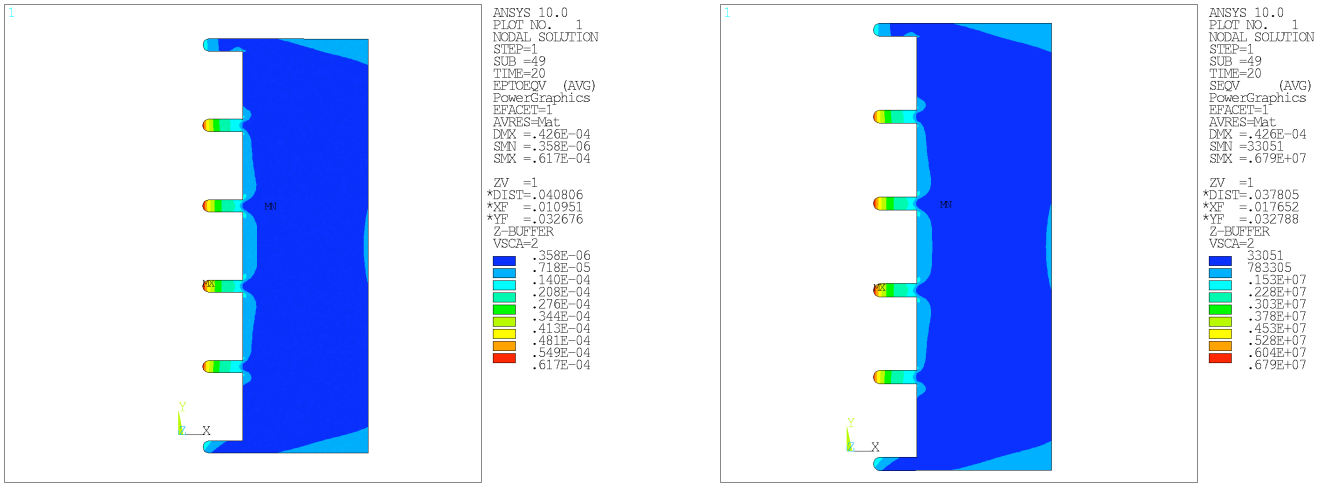

Figure 9: On the left: Von Mises Equivalent Stress [Pa]; On the right: Von Mises Equivalent Strain

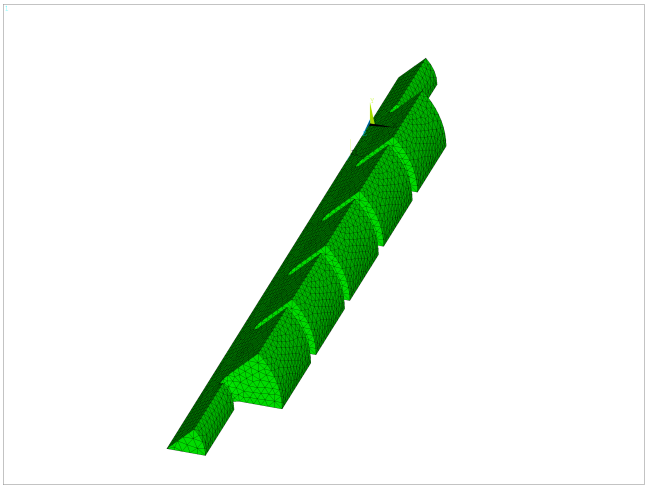

Figure 10: Element plot of the symmetric RF model

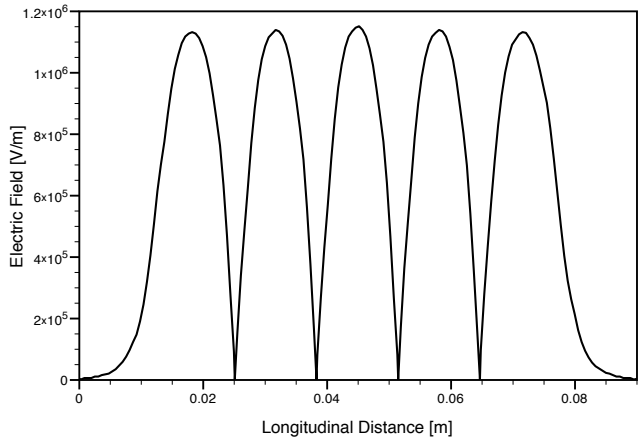

Figure 11: The π-mode (11.4 GHz). Axial profile of the Electric Field sum (module of the vector sum) [V/m]

5.3 Thermal Analysis Results

Coupling analysis means that the results of simulations in one domain are used as input for the other domain. In this case we meshed the copper cavity model and apply loads and boundary condition to it, after having deleted the previous elements corresponding to the vacuum space. Figure 5.3 shows the temperature profile in the whole cavity for 304.5 K external temperature, while in Figure 5.3, the radial profile on the two central irises (up-to the external boundary) is shown. The axial temperature distribution is similar to that induced by the thermal heater, even if in the radiation heating calculation we obtain a flatter temperature profile, with isothermal curves almost parallels to the cylindrical outer wall. In case of thermal load from power loss, the axial temperature profile is little more peaked in the middle with respect to the radiation case, with consequent larger temperature gradients in axial direction than that estimated in the radiation case (on the inner profile the longitudinal ΔT_{max} is about 0.65 K in the radiation heating case and 1.0 K in the RF case). The maximum radial temperature difference for both cases is detected in correspondence of the central irises and is about 2.6 K (see Figure 5) for the radiation case and 3.7 K (see Figure 5.3) for the RF case.

The temperature profiles shown in Figure 6 and 7 of paragraph §3 are to be compared with those generated in the cavity when the heating power is produced in the π-mode by the rf power loss in the skin depth along the inner surface (figure 16 and 15, respectively). If these profiles are close to each other both in shape and in the maximum axial and radial difference of temperature (within 30% could be sufficient), the proposed

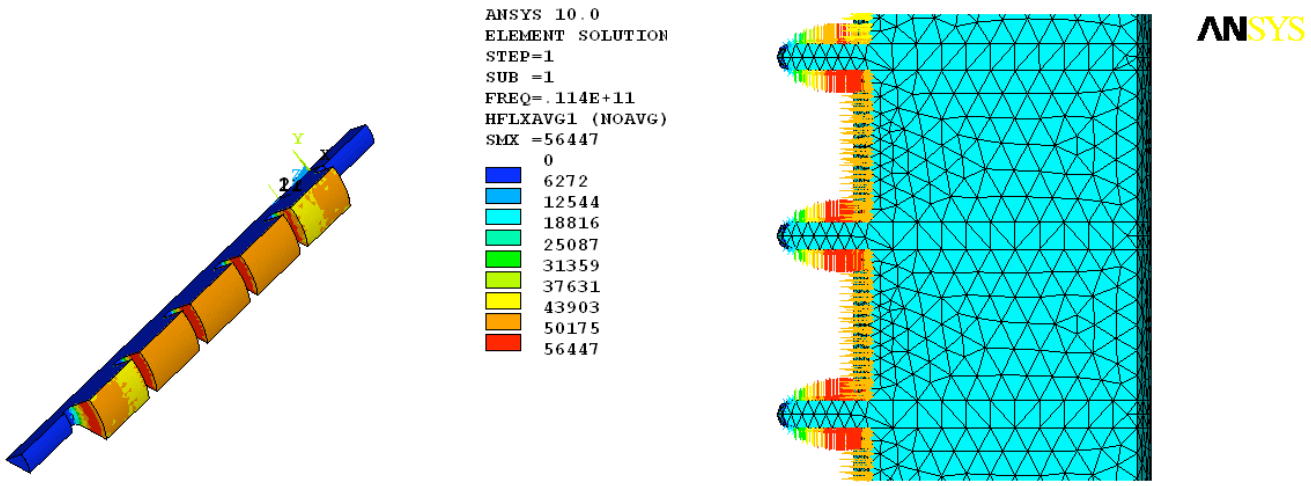

Figure 12: Heat Flux Intensities [W/m^2], due to Surface Power Loss, entering on the inner surface of the cavity

radiation heating method can be considered a reliable experimental way by which estimate and predict the mechanical deformations that the cavity undergoes when it is operating in the π-mode.

6 Conclusions

The aim of this work is to illustrate the use of a thermal radiator for testing the temperature distribution inside an X-band linac structure and to support the results by simulation with the ANSYS code. Experiments have been performed with such a radiator and the measured temperature distributions are compared with the computed ones. The result of this analysis is that the calculated values reproduce the experimental results with an accuracy of 20%, that is sufficient for checking the efficiency of the structure cooling design.

This work demonstrates that it is possible to use a thermal radiator for testing the temperature distribution in the structure. The computed stress and strain field inside the cavity allow to estimate how much the induced mechanical deformation can affect the frequency of the cavity. The code allows computing the stress and strain fields consequent to the temperature gradients. The structure deformations can be used to evaluate the frequency shifts of the cavity modes.

By exploiting the ability of the ANSYS code to link electromagnetic and thermal analyses, a further simulation has been done. A coupled-field analysis by a single code

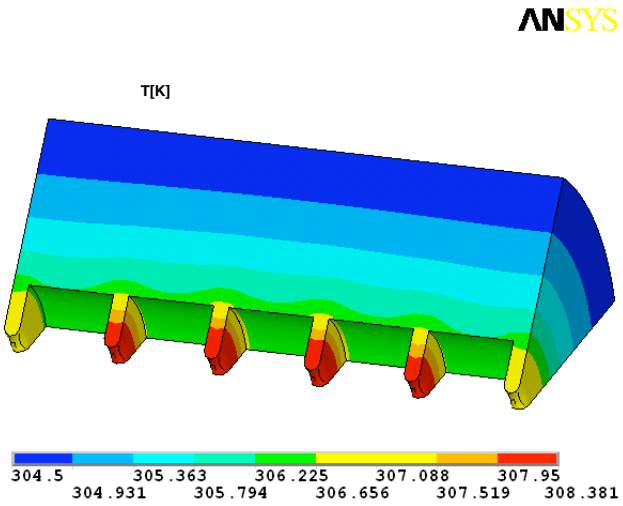

Figure 13: Temperature Profile in the copper cavity for a thermal load of 150 W and a boundary surface temperature equal to 304.5 K

allows to evaluate the RF losses and the consequent temperature distribution in the cavity with better accuracy than by the exchange of information between different simulators. It has been confirmed that the axial temperature distribution is similar to that induced by the thermal heater, even if some important differences have been detected and discussed.

Acknowledgments

The work is partly supported by Ministero Istruzione Università Ricerca, *Progetti Strategici*, DD 1834, Dec. 4, 2002 and European Contract RII3-CT-PHI506395CARE.

References

[1] D. Alesini et al.: “The SPARC Project: A High Brightness Electron Beam Source at LNF to Drive a SASE-FEL Experiment”, presented at PAC2003, 12-16/5/2003, Portland, Oregon, USA.

[2] S. Bini, P. Chimenti, V. Chimenti, R. Di Raddo, V. Lollo, B. Spataro, F. Tazzioli: ”Thermal Measurements on a RF 11,4 GHz Accelerating Structure”, RF-06/003, 29/09/2006

[3] ANSYS is a trademark of SAS Inc. www.ansys.com

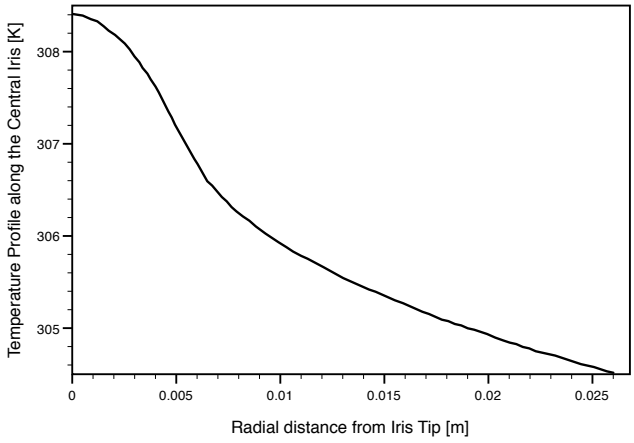

Figure 14: Radial Temperature Profile from the tip of the central irises to the external boundary, in case of rf excitation at the π-mode

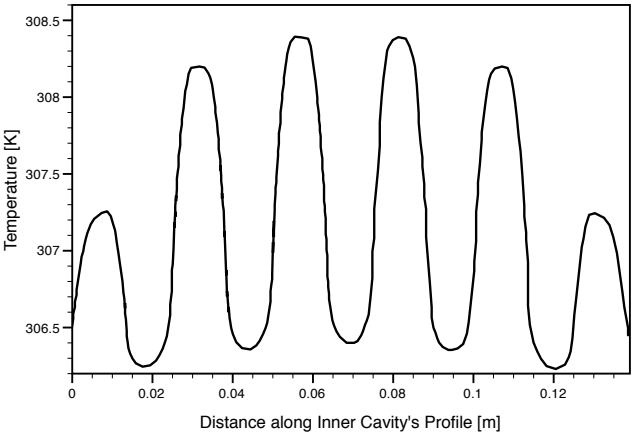

Figure 15: Axial Temperature Profile along the inner cavity's profile in case of rf excitation at the π-mode

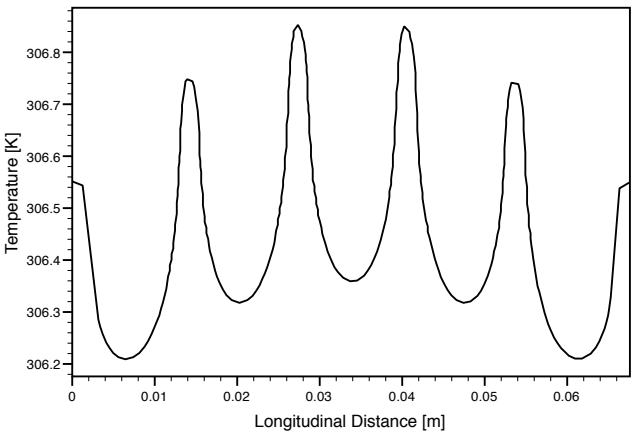

Figure 16: Axial Temperature Profile in the Cavity (along the diameter at the iris bases), in case of rf excitation at the π-mode